

Genomic Evolution and Personalized Therapy of an Infantile Fibrosarcoma Harboring an *NTRK* Oncogenic Fusion

Anne Thorwarth, MD¹; Kerstin Haase, PhD^{1,2,3,4,5}; Claudia Röefzaad, MSc^{1,2,3}; Kristian W. Pajtler, MD^{4,5,6,7}; Kathrin Schramm, PhD^{4,5,6,7}; Kathrin Hauptmann, MD⁸; Anke Behnke, PhD⁸; Christian Vokuhl, MD⁹; Thomas Elgeti, MD¹⁰; Alexander Gratopp, MD¹¹; Johannes H. Schulte, MD^{1,4,5}; Monika Scheer, MD¹; Pablo Hernáiz Driever, MD¹; Karsten Nysom, MD¹²; Angelika Eggert, MD^{1,4,5,13}; Anton G. Henssen, MD^{1,2,3,4,5}; and Hedwig E. Deubzer, MD^{1,2,3,4,5,13}

JCO Precis Oncol 6:e2100283. © 2022 by American Society of Clinical Oncology

Creative Commons Attribution Non-Commercial No Derivatives 4.0 License 

Introduction

Infantile fibrosarcomas are characterized by oncogenic fusions involving neurotrophic receptor tyrosine kinase genes (*NTRK1*, *NTRK2*, and *NTRK3*),¹ which cause expression of oncoproteins with increased tropomyosin receptor kinase (TRK) activity.² New TRK inhibitors such as larotrectinib are effective in the majority of patients with tumors expressing *NTRK* fusions including infantile fibrosarcoma.^{3,4} Secondary mutations within the ATP-binding pocket of the TRK kinase domain can lead to resistance to first-generation TRK inhibitors.² Second-generation TRK inhibitors such as selitrectinib can overcome such resistance.^{1,5} Mechanisms of resistance to second-generation TRK inhibitors are not well understood, and possible therapeutic strategies are largely lacking in these cases.

Case Report

The 13-month-old patient presented to an outside hospital with progressing respiratory insufficiency requiring invasive mechanical ventilation after transfer to the Charité—Universitätsmedizin Berlin. Imaging displayed a large right-sided intrathoracic mass (Fig 1). Histopathological evaluation of the first two biopsies remained inconclusive. Two cycles of neoadjuvant polychemotherapy were administered (N4 according to the NB2016 Registry⁶ and vincristine, actinomycin D, cyclophosphamide [VAC] according to the Cooperative Soft Tissue Sarcoma Study Group [CWS]⁷). Therapy response assessment according to the evaluation criteria for solid tumors, RECIST,⁸ demonstrated progressive disease (Fig 1). On the basis of a third biopsy (T1 [time point 1]), molecular pathology analysis classified the tumor as an *ETV6-NTRK3* fusion-positive infantile fibrosarcoma (Fig 2). The patient was enrolled in the phase I/II trial for the oral TRK inhibitor, larotrectinib,^{3,4,9,10} in pediatric patients with advanced solid or primary central nervous system

tumors (LOXO-101, BAY2757556; 100 mg/m² twice a day; ClinicalTrials.gov identifier: [NCT02637687](https://clinicaltrials.gov/ct2/show/study/NCT02637687)). Tumor volume decreased > 98% (from 45 × 34 × 26 mm diameter = 480 mL to 23 × 22 × 25 mm in diameter = 6 mL) after 2 months of larotrectinib treatment (Fig 1; Data Supplement). Progressive disease was detected after total larotrectinib treatment duration of 4 months that required chemotherapeutic intervention with three VAC cycles because of recurrent respiratory symptoms (Fig 1). The tumor continued to grow under chemotherapy (Fig 1). At the molecular level (T2 [time point 2]), single-nucleotide variant (SNV) analysis on the basis of whole-exome sequencing (WES) detected the *NTRK3* p.G623R mutation in one of two analyzed tumor regions (Fig 3), which produces a protein incapable of binding larotrectinib.^{11,12} The patient was enrolled in the phase I/II trial designed to test safety, tolerability, and efficacy of the oral second-generation TRK inhibitor, selitrectinib⁵ (LOXO-195, BAY2731954; ClinicalTrials.gov identifier: [NCT03215511](https://clinicaltrials.gov/ct2/show/study/NCT03215511)). A partial response was achieved after 2.5 months, at a dose level of 43 mg/m² selitrectinib twice daily, but disease progressed after 3 months (Fig 1; Data Supplement). Selitrectinib was increased to 58 mg/m² twice daily, but the tumor continued to grow (Fig 1). A gross total tumor resection requiring bilobectomy was performed (T3 [time point 3]), Fig 2, and selitrectinib was resumed postoperatively. Disease progression 6 weeks postsurgery was treated with two cycles of the CWS I²VAd regimen, to which the tumor partially responded (Fig 1). WES of T3 tumor tissue identified the xDFG motif p.G696A mutation^{3,12} in the *NTRK3* gene (Fig 3). Therapy resistance to monotherapy with first- and second-generation TRK inhibitors prompted us to increase selitrectinib to a dose level of 87 mg/m² twice daily and combine it with the mitogen-activated protein kinase (MEK) 1/2 inhibitor, trametinib (0.032 mg/kg once daily) as oncogenic *NTRK* fusions are known to mediate elevated RAS/MAPK/ERK signaling cascade activity.^{2,13} The patient has remained

ASSOCIATED CONTENT

Data Supplement

Author affiliations and support information (if applicable) appear at the end of this article.

Accepted on April 12, 2022 and published at ascopubs.org/journal/po on May 25, 2022; DOI <https://doi.org/10.1200/P0.21.00283>

free of disease progression on this two-drug combination for > 1 year. The safety profile of the two-drug combination selitrectinib/trametinib was favorable with no detectable evidence of organ toxicity.

Written informed parental consent was received before inclusion in the respective clinical studies. The two-drug combination selitrectinib/trametinib was initiated as individual treatment attempt after written informed parental consent was obtained. Selitrectinib was purchased through the compassionate use program of Bayer (Leverkusen, Germany). Bayer had provided written permission to administer their investigational

drug selitrectinib in combination with trametinib. Trametinib was administered as off-label use medication. Parental consent for the use of surplus biomaterial samples for research purposes is documented in the German Society of Pediatric Oncology and Hematology CWS registry. All clinical investigations were conducted in accordance with the Declaration of Helsinki. All clinical studies were approved by the appropriate institutional review boards. The investigators obtained written informed parental consent to publish this report. The details of molecular pathology analysis, tumor sequencing, and SNV and copy number variant analyses are supplied in the Data Supplement.¹⁴⁻²⁵

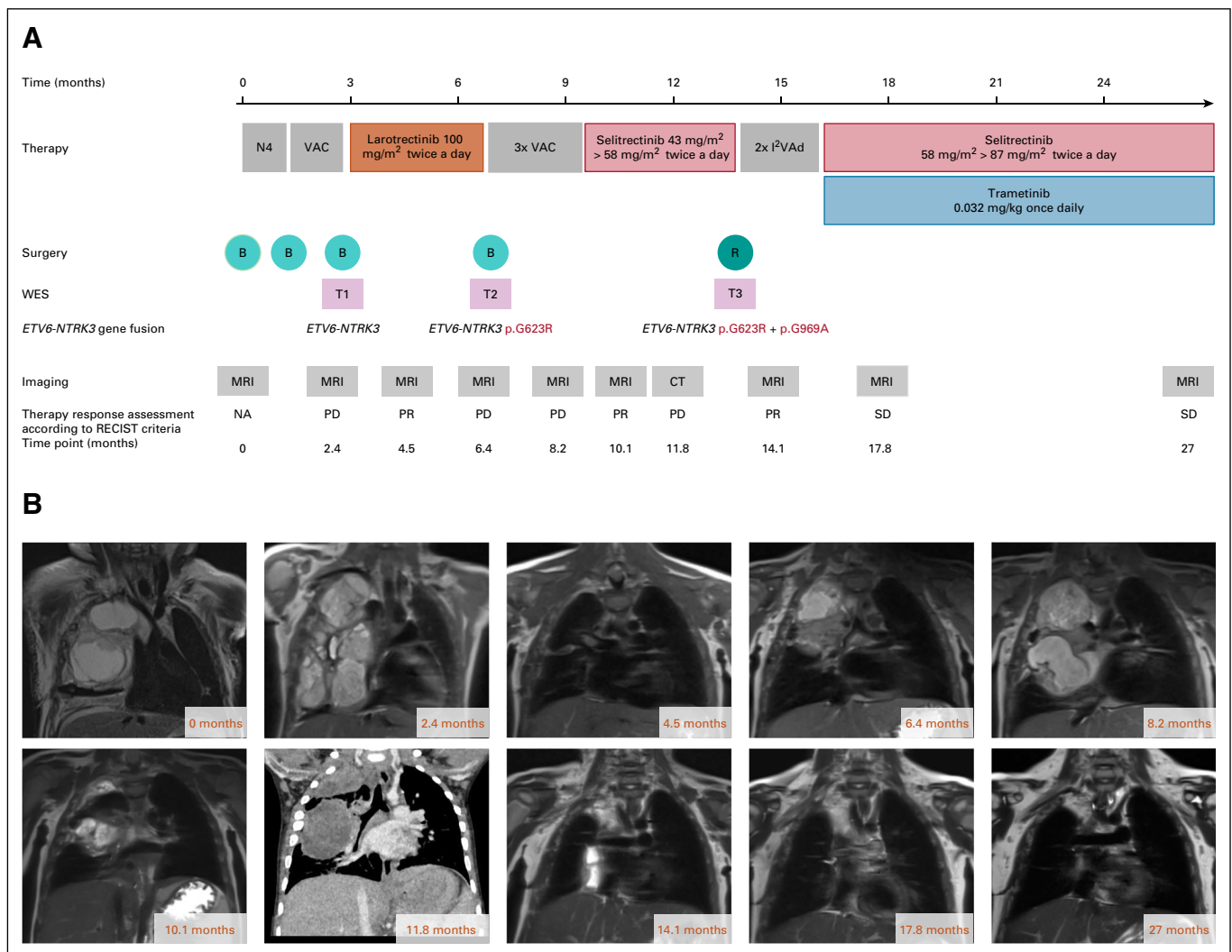


FIG 1. Treatment timeline and assessments. (A) Shown is the timeline of diagnosis and therapeutic interventions including drug therapies and surgery. Time points of whole exome sequencing studies and response evaluation by magnetic resonance imaging (MRI) and computed tomography (CT) scans in line with the response evaluation criteria in solid tumors (RECIST) are summarized below. (B) Shown are exemplarily selected images for each response evaluation time point. N4, chemotherapy regimen according to the NB2016 registry: doxorubicin, vincristine, cyclophosphamide; VAC, chemotherapy regimen according to the Cooperative Soft Tissue Sarcoma Study Group CWS of the German Society of Pediatric Oncology and Hematology (GPOH): vincristine, actinomycin-D, cyclophosphamide; I²VAd, chemotherapy regimen according to the Cooperative Soft Tissue Sarcoma Study Group CWS of the GPOH: ifosfamide, vincristine, doxorubicin; B, biopsy; R, resection; T, time point; n.a., not applicable; PD, progressive disease; PR, partial response; SD, stable disease; WES, whole exome sequencing.

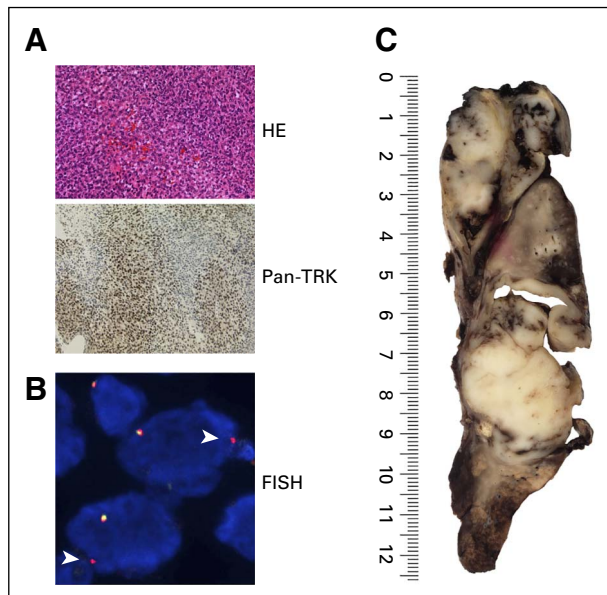


FIG 2. Overview of molecular pathology analysis. (A) H&E staining and pan-TRK immunohistochemistry were performed on formalin-fixed paraffin embedded tumor sections of the T1 tumor biopsy. (B) Dual color break apart FISH of interphase nuclei displayed one normal orange/green fusion signal and one orange signal (arrowed), indicating a chromosomal breakpoint and translocation of *ETV6*. Loss of the centromeric probe target (green) suggested additional genetic alterations. (C) Gross examination of the resected upper and middle pulmonary lobes, which were in large part taken by the infantile fibrosarcoma (90x50x30mm in maximum diameter). The cut surface of the tumor was whitish and had some hemorrhagic (<10%) and some necrotic areas (<10%). FISH, fluorescent in situ hybridization; HE, hematoxylin and eosin; TRK, tropomyosin receptor kinase.

Results

To characterize the genomic landscape of this infantile fibrosarcoma and define genetic alterations appearing under therapy, longitudinally collected tumor specimens were subjected to WES. SNV analysis of the T1 biopsy demonstrated two somatic mutations in cancer-related genes (*PIK3R1* p.F46_Q457del, *ARID1A* p.W1686Cfs*11; Fig 3). Spatial resolution was enabled at T2, in which only one tumor sample from the two regions harbored the solvent-front *NTRK3* p.G623R mutation¹¹ (Fig 3). No additional new mutations were detected in either tumor region, suggesting an otherwise stable genome (Fig 3). At T3, the xDFG motif *NTRK3* p.G696A mutation^{3,12} was detected (Fig 3). The G>R amino acid substitution (*NTRK3* residue 623) at time point T3 was caused by a G>C nucleotide substitution, whereas the samples at time point T2 showed variant read evidence of a G>A nucleotide substitution that also resulted in a G>R amino acid substitution, which may be indicative of parallel evolutionary changes (Fig 3). To analyze if the two nucleotide variants occurred on the same or on different alleles, we used a germline heterozygous single nucleotide polymorphism (SNP) located 99 bp downstream of the mutation in *NTRK3*. The G>C mutation in sample T3 was

phased to the T allele of the SNP. The G>A mutations in samples from the T2 biopsy had a very low frequency, and the samples had an overall lower coverage as T3. Thus, only two variant reads were phased with the aforementioned SNP. The mutation was also phased to the T allele of the SNP in both reads, indicating that both versions of the p.G623R mutation affect the same allele. A *CLTCL1* p.E1628D mutation was also detected at T3 (Fig 3). Copy number profiling in T1 and T3 samples revealed shared gains of chromosome 8 and parts of 6q as well as a loss of heterozygosity on chromosomes 15 and 16 (Fig 3). The only change in copy number at T3 was a whole chromosome 18 gain (Fig 3). RNA sequencing of the T3 sample and comparison with other sarcomas recorded in the INFORM registry demonstrated high-level *FGFR1*, *YES1*, and *CTLA4* expression that were considered borderline or very low-priority targets for precision treatment strategies (data not shown). We conclude that a stepwise acquisition of mutations in the *ETV6-NTRK3* fusion gene likely prevented effective inhibition of its oncogenic activity with first- and second-generation TRK inhibitors (schematic model of genomic tumor evolution in Fig 3).

Discussion

We here report on a patient with an *ETV6-NTRK3*-driven infantile fibrosarcoma that developed resistance to first- and second-generation TRK inhibitors. The tumor rapidly responded to larotrectinib monotherapy but acquired resistance through an *NTRK3* solvent-front mutation. Resistance was overcome with selitrectinib monotherapy, but an *NTRK3* xDFG motif mutation again rendered the disease refractory. As exemplified by this patient, treatment with first- and second-generation TRK inhibitors can elicit rapid and strong responses in the treatment-naïve and acquired resistant disease settings. The sequencing data reported provide no evidence to support a model of primary resistance. The reduction in tumor volume by > 98% after 2 months of larotrectinib treatment is in line with the reported *NTRK3* wild-type sequence at time point T1. Whether single-cell sequencing approaches of multiregion biopsies collected at initial diagnosis will unravel so far undetected *NTRK3* mutations that render the disease primarily resistant to monotherapy with TRK inhibitors remains to be investigated.

Although sustainable responses to TRK inhibition exist,^{3,4,9,10} the sequential acquisition of two *NTRK3* mutations under therapy pressure reported here demonstrates that close disease monitoring is warranted. Cross-sectional imaging studies are the current gold standard for monitoring intrathoracic lesions. Although this patient was monitored on a monthly basis, stepwise acquisition of resistance to first- and second-generation TRK inhibitor therapy resulted in rapid progressive disease that required intensive care measures. Whether liquid biopsy-based diagnostics²⁶ can better support resistance monitoring, therapy decisions, and response evaluation for tumors harboring oncogenic *NTRK3* fusions remains an open question. Increasing evidence suggests

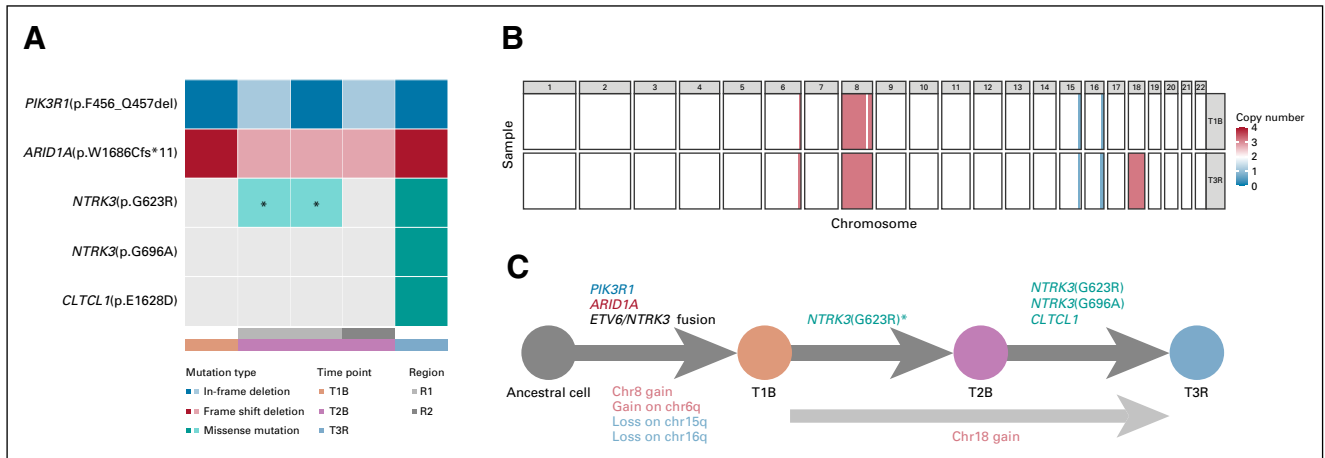


FIG 3. Molecular profiling of multi-sample sequencing data. (A) Mutation data derived from WES. Shown are all samples with an average coverage of more than 40X. Mutations were filtered against the cosmic cancer gene census v91³⁷. Only variants with a variant allele frequency above 10%, no variant reads in the matched normal and a predicted functional impact of moderate or high are shown. Darker colors indicate mutations that have been called by MuTect2³⁵, lighter shades represent variants that had supporting reads upon detailed inspection. The *NTRK3* G>R mutation at time point T3 is caused by a G>C mutation on the nucleotide level, whereas the samples marked with an asterisk, show variant read evidence of a G>A mutation that also results in a G>R amino acid exchange. (B) Copy number profiles for samples T1 and T3. Genomic segments are colored based on their absolute copy number. Diploid regions are shown in white, losses in shades of blue, gains in red. Only events affecting segments of 5MB or larger are shown. (C) Time line representing the order of events leading from the ancestral cell to the last analyzed tumor sample. SNVs and fusion events are shown above the time line, copy number variants beneath it. The coloring of individual events is consistent with panels A) and B). B, biopsy; R, resection; T, time point.

that follow-up using liquid biopsies is feasible for patients with fusion-positive sarcomas.^{27,28}

The primary mutational spectrum in this infantile fibrosarcoma was very low, with only two mutations detected in cancer-related genes. The *PIK3R1* gene affected by an in-frame deletion encodes for the p85 regulatory subunit of phosphoinositide 3-kinases, which regulate signaling pathways important for cell proliferation, survival, adhesion, and motility.²⁹ *PI3K* mutations have been linked to cancer,³⁰ primary immunodeficiencies,³¹ and developmental disorders.³² The *ARID1A* gene affected by a frameshift deletion is part of the SWItch/Sucrose Non-Fermentable (SWI/SNF) chromatin remodeling complex regulating eukaryotic gene expression. SWI/SNF complex mutations occur in 20% of human cancers, and *ARID1A* has the highest mutation rate across all SWI/SNF complex components.³³ *ARID1A* mutations were shown to be negatively associated with checkpoint immunotherapy responses and patient survival in different cancer entities.³⁴ The only mutation occurring under therapy affected the *CLTCL1* gene, a member of the clathrin heavy chain family

required for mitotic progression and cytokinesis.³⁵ *CLTCL1* mutations have been reported in oral and lung squamous cell carcinoma,^{36,37} meningioma,³⁸ and a rare case of thyroid follicular dendritic cell sarcoma.³⁹ The newly occurring copy number alterations detected at T3 may be attributable to the *CLTCL1* mutation-induced impairment of mitotic spindle stabilization. Altogether, genomic profiling in temporal and spatial resolution of this infantile fibrosarcoma identified a very low number of cancer-related, but undruggable, mutations. The borderline priority of all three overexpressed genes (*FGFR1*, *YES1*, and *CTLA4*) and the exhausted chemotherapeutic options prompted us to turn to downstream signaling cascades of the oncogenic *NTRK3* p.G623R p.G696R fusion protein, which include PI3K, RAS/MAPK/ERK, and PLCG1/PLCG2.¹³ Combining selitrectinib with trametinib, to also inhibit MEK1/MEK2 activity, resulted in > 1 year free of disease progression, thus providing insights into precision medicine strategies under conditions of acquired resistance to first- and second-generation TRK inhibition.

AFFILIATIONS

¹Department of Pediatric Hematology and Oncology, Charité—Universitätsmedizin Berlin, Corporate Member of Freie Universität Berlin and Humboldt-Universität Berlin, Berlin, Germany

²Experimental and Clinical Research Center (ECRC) of the Charité and the Max-Delbrück-Center for Molecular Medicine (MDC) in the Helmholtz Association, Berlin, Germany

³Max-Delbrück-Center for Molecular Medicine (MDC) in the Helmholtz Association, Berlin, Germany

⁴German Cancer Research Center (DKFZ), Heidelberg, Germany

⁵German Cancer Consortium (DKTK), Partner Sites Berlin and Heidelberg, Germany

⁶Department of Pediatric Hematology and Oncology, University Hospital Heidelberg, Heidelberg, Germany

⁷Hopp Children's Cancer Center Heidelberg (KiTZ), Heidelberg, Germany

⁸Institute of Pathology, Charité—Universitätsmedizin Berlin, Corporate Member of Freie Universität Berlin and Humboldt-Universität Berlin, Berlin, Germany

⁹Section of Pediatric Pathology, Institute of Pathology, University Hospital Bonn, Bonn, Germany

¹⁰Department of Radiology (including Pediatric Radiology), Charité-Universitätsmedizin Berlin, Corporate Member of Freie Universität Berlin and Humboldt-Universität Berlin, Berlin, Germany

¹¹Department of Pediatric Pulmonology, Immunology and Intensive Care Medicine, Charité—Universitäts-Medizin Berlin, Corporate Member of Freie Universität Berlin and Humboldt-Universität Berlin, Berlin, Germany

¹²Department of Pediatrics and Adolescent Medicine, Juliane Marie Centre, Rigshospitalet, Copenhagen University Hospital, Copenhagen, Denmark

¹³Berliner Institut für Gesundheitsforschung (BIH), Berlin, Germany

CORRESPONDING AUTHOR

Hedwig E. Deubzer, MD, Department of Pediatric Hematology and Oncology, Charité—Universitätsmedizin Berlin, Augustenburger Platz 1, 13353 Berlin, Germany; e-mail: hedwig.deubzer@charite.de.

SUPPORT

A.G.H. is supported by the *Deutsche Forschungsgemeinschaft* (DFG, German Research Foundation)—398299703 and the European Research Council (ERC) under the European Union's Horizon 2020 research and innovation program (Grant Agreement No. 949172). H.E.D. is supported by the Advanced Clinician Scientist Program funded by the Charité—University Medicine Berlin and the Berliner Institut für Gesundheitsforschung (BIH) and by the European Union through TRANSCAN-2/LIQUIDHOPE (01KT1902). K.H., J.H.S., A.E., A.G.H., and H.E.D. are supported by the German Cancer Research Consortium (DKTK), partner site Berlin.

AUTHOR CONTRIBUTIONS

Conception and design: Anne Thorwarth, Angelika Eggert, Anton G. Henssen, Hedwig E. Deubzer

Financial support: Hedwig E. Deubzer

Administrative support: Angelika Eggert, Hedwig E. Deubzer

Provision of study materials or patients: Christian Vokuhl, Pablo Hernáiz Driever, Karsten Nysom, Angelika Eggert, Hedwig E. Deubzer

Collection and assembly of data: Anne Thorwarth, Claudia Röefzaad, Kristian W. Pajtler, Kathrin Hauptmann, Anke Behnke, Christian Vokuhl, Thomas Elgeti, Johannes H. Schulte, Pablo Hernáiz Driever, Anton G. Henssen, Hedwig E. Deubzer

Data analysis and interpretation: Anne Thorwarth, Kerstin Haase, Kristian W. Pajtler, Kathrin Schramm, Christian Vokuhl, Thomas Elgeti, Alexander Gratopp, Monika Scheer, Pablo Hernáiz Driever, Karsten Nysom, Anton G. Henssen, Hedwig E. Deubzer

Manuscript writing: All authors

Final approval of manuscript: All authors

Accountable for all aspects of the work: All authors

AUTHORS' DISCLOSURES OF POTENTIAL CONFLICTS OF INTEREST

The following represents disclosure information provided by authors of this manuscript. All relationships are considered compensated unless otherwise noted. Relationships are self-held unless noted. I = Immediate Family Member, Inst = My Institution. Relationships may not relate to the subject matter of this manuscript. For more information about ASCO's conflict of interest policy, please refer to www.asco.org/rwc or ascopubs.org/po/author-center.

Open Payments is a public database containing information reported by companies about payments made to US-licensed physicians (Open Payments).

Karsten Nysom

Honoraria: Y-mAbs Therapeutics

Consulting or Advisory Role: Bayer, EUSA Pharma, Y-mAbs Therapeutics Inc

Travel, Accommodations, Expenses: Bayer

Anton G. Henssen

Research Funding: Bayer

No other potential conflicts of interest were reported.

ACKNOWLEDGMENT

The authors thank Kathy Astrahantseff for critical reading of the manuscript.

REFERENCES

- Shulman DS, DuBois SG: The evolving diagnostic and treatment landscape of NTRK-fusion-driven pediatric cancers. *Paediatr Drugs* 22:189-197, 2020
- Cocco E, Scaltriti M, Drilon A: NTRK fusion-positive cancers and TRK inhibitor therapy. *Nat Rev Clin Oncol* 15:731-747, 2018
- Drilon A, Laetsch TW, Kummar S, et al: Efficacy of larotrectinib in TRK fusion-positive cancers in adults and children. *N Engl J Med* 378:731-739, 2018
- Laetsch TW, DuBois SG, Mascarenhas L, et al: Larotrectinib for paediatric solid tumours harbouring NTRK gene fusions: Phase 1 results from a multicentre, open-label, phase 1/2 study. *Lancet Oncol* 19:705-714, 2018
- Drilon A, Nagasubramanian R, Blake JF, et al: A next-generation TRK kinase inhibitor overcomes acquired resistance to prior TRK kinase inhibition in patients with TRK fusion-positive solid tumors. *Cancer Discov* 7:963-972, 2017
- Simon T, Hero B, Schulte JH, et al: 2017 GPOH guidelines for diagnosis and treatment of patients with neuroblastic tumors. *Klin Padiatr* 229:147-167, 2017
- Sparber-Sauer M, Vokuhl C, Seitz G, et al: The impact of local control in the treatment of children with advanced infantile and adult-type fibrosarcoma: Experience of the cooperative weichteilsarkom studien-gruppe (CWS). *J Pediatr Surg* 55:1740-1747, 2020
- Eisenhauer EA, Therasse P, Bogaerts J, et al: New response evaluation criteria in solid tumours: Revised RECIST guideline (version 1.1). *Eur J Cancer* 45:228-247, 2009
- DuBois SG, Laetsch TW, Federman N, et al: The use of neoadjuvant larotrectinib in the management of children with locally advanced TRK fusion sarcomas. *Cancer* 124:4241-4247, 2018
- Hong DS, DuBois SG, Kummar S, et al: Larotrectinib in patients with TRK fusion-positive solid tumours: A pooled analysis of three phase 1/2 clinical trials. *Lancet Oncol* 21:531-540, 2020
- Drilon A, Li G, Dogan S, et al: What hides behind the MASC: Clinical response and acquired resistance to entrectinib after ETV6-NTRK3 identification in a mammary analogue secretory carcinoma (MASC). *Ann Oncol* 27:920-926, 2016
- Kheder ES, Hong DS: Emerging targeted therapy for tumors with NTRK fusion proteins. *Clin Cancer Res* 24:5807-5814, 2018
- Khotskaya YB, Holla VR, Farago AF, et al: Targeting TRK family proteins in cancer. *Pharmacol Ther* 173:58-66, 2017

14. Csanyi-Bastien M, Lanic MD, Beaussire L, et al: Pan-TRK immunohistochemistry is highly correlated with NTRK3 gene rearrangements in salivary gland tumors. *Am J Surg Pathol* 45:1487-1498, 2021
15. Worst BC, van Tilburg CM, Balasubramanian GP, et al: Next-generation personalised medicine for high-risk paediatric cancer patients—The INFORM pilot study. *Eur J Cancer* 65:91-101, 2016
16. Martin M: Cutadapt removes adapter sequences from high-throughput sequencing reads. *EMBnet J* 17:10-12, 2011
17. Li H: Aligning sequence reads, clone sequences and assembly contigs with BWA-MEM. *ArXiv*, 2013 [10.48550/arXiv.1303.3997](https://arxiv.org/abs/10.48550/arXiv.1303.3997)
18. van der Auwera GA, O'Connor BD: *Genomics in the Cloud: Using Docker, GATK, and WDL in Terra*. Sebastopol, CA, O'Reilly Media, Incorporated, 2020
19. Li H, Handsaker B, Wysoker A, et al: The sequence alignment/map format and SAMtools. *Bioinformatics* 25:2078-2079, 2009
20. Van der Auwera GA, Carneiro MO, Hartl C, et al: From FastQ data to high confidence variant calls: The Genome Analysis Toolkit best practices pipeline. *Curr Protoc Bioinformatics* 43:11.10.1-11.10.33, 2013
21. Benjamin D, Sato T, Cibulskis K, et al: Calling somatic SNVs and indels with Mutect2. *bioRxiv*, 2019 [10.1101/861054](https://doi.org/10.1101/861054)
22. McLaren W, Gil L, Hunt SE, et al: The ensembl variant effect predictor. *Genome Biol* 17:122, 2016
23. Tate JG, Bamford S, Jubb HC, et al: COSMIC: The catalogue of somatic mutations in cancer. *Nucleic Acids Res* 47:D941-D947, 2019
24. Clarke L, Fairley S, Zheng-Bradley X, et al: The international genome sample resource (IGSR): A worldwide collection of genome variation incorporating the 1000 genomes project data. *Nucleic Acids Res* 45:D854-D859, 2017
25. Van Loo P, Nordgard SH, Lingjaerde OC, et al: Allele-specific copy number analysis of tumors. *Proc Natl Acad Sci USA* 107:16910-16915, 2010
26. Van Paemel R, Vlug R, De Preter K, et al: The pitfalls and promise of liquid biopsies for diagnosing and treating solid tumors in children: A review. *Eur J Pediatr* 179:191-202, 2020
27. Krumbholz M, Hellberg J, Steif B, et al: Genomic EWSR1 fusion sequence as highly sensitive and dynamic plasma tumor marker in ewing sarcoma. *Clin Cancer Res* 22:4356-4365, 2016
28. Hayashi M, Chu D, Meyer CF, et al: Highly personalized detection of minimal Ewing sarcoma disease burden from plasma tumor DNA. *Cancer* 122:3015-3023, 2016
29. Vivanco I, Sawyers CL: The phosphatidylinositol 3-Kinase AKT pathway in human cancer. *Nat Rev Cancer* 2:489-501, 2002
30. Samuels Y, Wang Z, Bardelli A, et al: High frequency of mutations of the PIK3CA gene in human cancers. *Science* 304:554, 2004
31. Lucas CL, Chandra A, Nejentsev S, et al: PI3Kdelta and primary immunodeficiencies. *Nat Rev Immunol* 16:702-714, 2016
32. Dymont DA, Smith AC, Alcantara D, et al: Mutations in PIK3R1 cause SHORT syndrome. *Am J Hum Genet* 93:158-166, 2013
33. Kadoch C, Hargreaves DC, Hodges C, et al: Proteomic and bioinformatic analysis of mammalian SWI/SNF complexes identifies extensive roles in human malignancy. *Nat Genet* 45:592-601, 2013
34. Li J, Wang W, Zhang Y, et al: Epigenetic driver mutations in ARID1A shape cancer immune phenotype and immunotherapy. *J Clin Invest* 130:2712-2726, 2020
35. Niswonger ML, O'Halloran TJ: A novel role for clathrin in cytokinesis. *Proc Natl Acad Sci USA* 94:8575-8578, 1997
36. Al-Hebshi NN, Li S, Nasher AT, et al: Exome sequencing of oral squamous cell carcinoma in users of Arabian snuff reveals novel candidates for driver genes. *Int J Cancer* 139:363-372, 2016
37. Li S, Wang L, Ma Z, et al: Sequencing study on familial lung squamous cancer. *Oncol Lett* 10:2634-2638, 2015
38. Lyu J, Quan Y, Wang JB, et al: Whole exome sequencing of multiple atypical meningiomas in a patient without history of neurofibromatosis type II: A case report. *Am J Case Rep* 21:e923928, 2020
39. Davila JI, Starr JS, Attia S, et al: Comprehensive genomic profiling of a rare thyroid follicular dendritic cell sarcoma. *Rare Tumors* 9:6834, 2017

